Published online 17 July 2010 *Nucleic Acids Research, 2010, Vol. 38, No. 21* ***7791–7799***
doi:10.1093/nar/gkq627

Structural insights into the function of aminoglycoside-resistance A1408 16S rRNA methyltransferases from antibiotic-producing and human pathogenic bacteria

Rachel Macmaster[1,2], Natalia Zelinskaya[1], Miloje Savic[1], C. Robert Rankin[1] and Graeme L. Conn[1,*]

[1]Department of Biochemistry, Emory University School of Medicine, Atlanta GA 30322, USA and [2]Manchester Interdisciplinary Biocentre, Faculty of Life Sciences, University of Manchester, Manchester M1 7DN, UK

Received April 16, 2010; Revised June 11, 2010; Accepted June 29, 2010

ABSTRACT

X-ray crystal structures were determined of the broad-spectrum aminoglycoside-resistance A1408 16S rRNA methyltransferases KamB and NpmA, from the aminoglycoside-producer *Streptoalloteichus tenebrarius* and human pathogenic *Escherichia coli*, respectively. Consistent with their common function, both are Class I methyltransferases with additional highly conserved structural motifs that embellish the core SAM-binding fold. In overall structure, the A1408 rRNA methyltransferase were found to be most similar to a second family of Class I methyltransferases of distinct substrate specificity (m^7G46 tRNA). Critical residues for A1408 rRNA methyltransferase activity were experimentally defined using protein mutagenesis and bacterial growth assays with kanamycin. Essential residues for SAM coenzyme binding and an extended protein surface that likely interacts with the 30S ribosomal subunit were thus revealed. The structures also suggest potential mechanisms of A1408 target nucleotide selection and positioning. We propose that a dynamic extended loop structure that is positioned adjacent to both the bound SAM and a functionally critical structural motif may mediate concerted conformational changes in rRNA and protein that underpin the specificity of target selection and activation of methyltransferase activity. These new structures provide important new insights that may provide a starting point for strategies to inhibit these emerging causes of pathogenic bacterial resistance to aminoglycosides.

INTRODUCTION

Bacterial antibiotic resistance is a major contemporary clinical challenge that demands urgent studies of the activities and origins of resistance determinants. A variety of mechanisms, often found in combination, confer resistance by reducing the effective drug concentration in the cell by transport or modification, or altering the drug binding site through mutation or chemical modification (1).

The protein translation machinery is the target of many classes of antibacterial agents. For example, aminoglycoside antibiotics bind to the 30S ribosomal subunit A site, inducing errors in decoding, occluding the mRNA path or inhibiting mRNA:tRNA translocation (2). These diverse molecules can be collected into three broad groups: the 4,6-disubstituted deoxystreptamines (4,6-DOS) including kanamycin, tobramycin and gentamicin; the 4,5-disubstituted deoxystreptamines (4,5-DOS) such as paromomycin and neomycin; and a third more diverse group with alternative cores or ring arrangements, such as apramycin or streptomycin. Two families of *S*-adenosyl-L-methionine (SAM)-dependent aminoglycoside-resistance methyltransferases act upon 16S rRNA to produce either an N7-methyl G1405 (m^7G1405) or N1-methyl A1408 (m^1A1408) modification. Whereas the resistance spectrum conferred by m^7G1405 is

*To whom correspondence should be addressed. Tel: +1 404 727 5965; Fax: +1 404 727 2738; Email: gconn@emory.edu
Present address:
C. Robert Rankin, Department of Pathology and Laboratory Medicine, Biochemistry, Cell and Developmental Biology Program, Emory University, Atlanta, GA, USA.

limited to the 4,6-DOS aminoglycosides (e.g. kanamycin and gentamicin), the m^1A1408 modification confers a broad resistance spectrum that includes examples of the 4,6-DOS (e.g. kanamycin but not gentamicin) and 4,5-DOS aminoglycoside groups and also apramycin (3).

The G1405 and A1408 16S rRNA aminoglycoside-resistance methyltransferases were first identified in antibiotic producing bacteria, where they act to protect against self-intoxication (4). However, they are now increasingly being identified in both animal and human pathogens (5,6). The transfer and world-wide dissemination among pathogenic bacterial populations of the Erm methyltransferases, that methylate A2058 of 23S rRNA to confer a Macrolide–Lincosamide–Streptogramin B (MLS_B) resistance phenotype, severely restricts the clinical utility of these drugs (7). The recent identification of pathogen aminoglycoside-resistance 16S rRNA methyltransferases, often associated with mobile genetic elements, suggests that the aminoglycoside family of antibiotics is now similarly threatened by the increasing prevalence of these enzymes (8,9).

Recent bioinformatic analysis and modeling of the A1408 methyltransferase KamB from *Streptoalloteichus hindustanus* identified an adjustment to the 5′-end of the open reading frame that would be required to produce an intact Class I methyltransferase SAM-binding fold (10). This observation facilitated the first recombinant expression of a KamB protein in our laboratory (3). These studies provided initial experimental verification that the A1408 methyltransferases are indeed members of the Class I methyltransferases, a large group that modify diverse substrates including numerous rRNA, tRNA, DNA and many small molecules (11). Substrate specificity in these enzymes is thought to arise through the varied embellishments to the core fold which can be present at either terminus or in the loops between core β-strands.

In addition to the Kam family of four distinct A1408 methyltransferases from aminoglycoside-producers, one confirmed enzyme of apparently identical function, NpmA, has been identified in human pathogenic *Escherichia coli* (ARS3) from a clinical isolate (9). Phylogenetic analysis also clusters CmnU and Kmr from the capreomycin-producer *Saccharothrix mutabilis* subsp. *capreolus* (12) and the cellulose degrading bacterium *Sorangium cellulosum* (13), respectively, and two additional hypothetical proteins with the five known A1408 methyltransferases (Supplementary Figure S1). However, these enzymes have not been demonstrated to possess A1408 methyltransferase activity. Inference of such activity from sequence information in the absence of functional characterization must be made with caution since sequence identity is relatively low even among the five confirmed A1408 rRNA methyltransferases. Most importantly, the critical structures outside of the core SAM-binding fold and the specific residues that define the A1408 methyltransferase activity are not known.

Here, we describe the high-resolution crystal structures and functional analysis of KamB from the nebramycin producer *Streptoalloteichus tenebrarius* (14,15) and its pathogen ortholog NpmA (9). With recent reports of two complete structures of the G1405 methyltransferases, RmtB (16) and Sgm (17), a complete structural characterization of both enzyme families from both aminoglycoside producer and pathogenic bacteria is now available. Our studies provide new insights into the likely molecular mechanisms of action of the A1408 methyltransferases, and reveal unexpected structural similarities outside of the core Class I methyltransferase fold to another RNA methyltransferase family of different target nucleotide modification (m^7G) and substrate specificity (tRNA).

MATERIALS AND METHODS

Protein crystallization and structure determination

KamB and NpmA proteins were overexpressed in strain BL21(DE3) from pET44 plasmid constructs containing *E. coli* optimized genes produced by chemical synthesis (GeneArt). Selenomethionine KamB was also overexpressed in strain BL21(DE3) using Overnight Express (Novagen) autoinduction media supplemented with 30 mg/l seleno-L-methionine. All proteins were purified to homogeneity using the same two-step procedure involving heparin affinity and gel filtration chromatographies (N.V.Zelinskaya *et al.*, submitted for publication).

Crystallization was performed by sitting drop vapor diffusion at 20°C using KamB or NpmA (10 mg/ml) with 1 mM SAM in Tris buffer (pH 8.0 and 7.0, respectively) and 150 mM NaCl. KamB crystals were grown in Tris–HCl buffer pH 8.0 containing 250 mM KSCN and 24% polyethylene glycol (PEG) 2000 monomethylether, and cryoprotected using the same conditions supplemented with 25% PEG 400. NpmA crystals were grown in 100 mM HEPES buffer pH 7.5 with 14% PEG 6000 and 4% MPD and adequate cryoprotection was achieved by increasing the MPD to final 25% concentration. All diffraction data were collected at the Advanced Photon Source SER-CAT beamline BM-22 and processed using HKL2000 (18). Single wavelength anomalous diffraction (SAD) data for experimental phasing using selenomethionine-KamB was collected at 0.97911 Å (selenium K edge peak).

Identification of the selenium sites and initial model building of KamB was performed using Phenix (19) with further automated building using ARP/wARP (20) and manual building in Coot (21) to complete the structure. The core KamB SAM-binding domain structure was used as a molecular replacement model in Phaser (22), and the NpmA structure completed using Coot (21). Refinement of both structures against high resolution native data was performed using Phenix (23), employing TLS refinement in the final stages (24). Complete data collection and processing and structure refinement statistics are provided in Table 1.

Analysis of KamB protein fold similarity to other protein structures was performed using the DALI server (25). Modeling of potential A1408 interactions with KamB was performed using HADDOCK (26).

Mutagenesis and MIC assays

Site-directed mutagenesis of KamB was performed in the pQE30 vector (Qiagen) using the QuikChange Lightning

Table 1. Complete X-ray data collection and structure refinement statistics

	SeMet KamB	KamB–SAH	NpmA–SAM
Space group	*P*21	*P*21	*P*21
Resolution (Å)	2.00	1.69	1.80
Cell dimensions			
a, *b*, *c* (Å)	48.6, 64.2, 71.6	48.3, 64.1, 72.0	49.7, 59.8, 91.7
α, β, γ (°)	90, 104.1, 90	90.0, 104.6, 90.0	90, 96.3, 90
Wavelength	0.97911(*Peak*)	1.0	1.0
Resolution (Å)[a]	50–2.0 (2.07–2.0)	50–1.69 (1.75–1.69)	50–1.80 (1.87–1.80)
R_{merge}[b]	0.169 (0.501)	0.05 (0.285)	0.067 (0.395)
$I/\sigma I$	17.4 (6.3)	16.8 (3.4)	20 (3.4)
Completeness (%)	100 (100)	99.1 (92.0)	99.9 (99.7)
Redundancy	9.9 (9.0)	3.8 (3.6)	4.6 (4.3)
Figure of Merit[c]	0.31	–	–
No. reflections		46 638	49 392
R_{work}/R_{free}[d]		17.2/20.2	17.8/20.6
Number of atoms			
Protein		3431	3621
Ligand/ion		52	54
Water		283	242
B-factors			
Protein		19.89	29.43
Ligand/ion		15.91	28.44
Water		25.92	35.69
Ramachandran Plot			
Favorable (%)		99.1	98.9
Allowed (%)		0.9	1.1
R.m.s. deviations			
Bond lengths (Å)		0.006	0.007
Bond angles (°)		1.108	1.050

[a]Values in parenthesis are for the highest resolution shell.
[b]$R_{merge} = \Sigma hkl\ \Sigma i|Ii\ (hkl) - \langle I(hkl)\rangle|/\Sigma hkl\ \Sigma i\ Ii(hkl)$.
[c]Figure of merit (FoM) $m = \cos\{\alpha - \alpha(best)\}$
[d]$R_{work} = \Sigma hkl|F_o\ (hkl) - F_c\ (hkl)|/\Sigma hkl|\ F_o\ (hkl)$, where F_o and F_c are observed and calculated structure factors, respectively. R_{free}, applies to the 5% of reflections chosen at random to constitute the test set.

kit (Stratagene). Minimum inhibitory concentrations (MIC) of kanamycin were measured in liquid culture for *E. coli* BL21(DE3) transformed with empty pQE30 vector or pQE30 encoding wild-type or mutant KamB proteins. Initial cultures for each experiment were grown to saturation in LB medium supplemented with 50 mg/ml ampicillin. Fresh LB medium (10 ml) containing various concentrations of kanamycin (0–1200 μg/ml) was inoculated at 1:1000 dilution using each starter culture and incubated at 37°C for 16 h with vigorous shaking. Assays were performed at least in triplicate and the MIC was defined as the lowest concentration of kanamycin for which no growth could be detected ($A_{600} < 0.05$).

RESULTS

Crystal structures of KamB–SAH and NpmA–SAM complexes

KamB (215 amino acids) was crystallized in the presence of SAM and the complex structure determined at 1.69 Å using experimentally determined phases (Table 1). NpmA (219 amino acids) was also co-crystallized with SAM and its structure determined to 1.8 Å by molecular replacement using our KamB structure as a model. Both structures were refined with good statistics (Table 1). In both crystals, the asymmetric unit contained two molecules with clear continuous density allowing modeling of all amino acids in both copies of KamB and NpmA. The bound SAM molecule was clearly defined in the NpmA–SAM complex (Figure 1A). For KamB, coenzyme was present at partial occupancy and the absence of any density for the methyl group suggested that the methylation reaction by-product S-adenosylhomocysteine (SAH) was present, as previously observed in crystal structures of other rRNA methyltransferases crystallized in the presence of SAM (16,27).

The structures of KamB and NpmA (Figure 1B and C) definitively confirm both as Class I methyltransferase enzymes that possess a characteristic Rossmann-like SAM-binding fold of a seven-stranded β-sheet with central topological switch point (6↑7↓5↑4↑•1↑2↑3↑) flanked by α-helices (11). KamB and NpmA are also essentially identical in the N-terminal domain and extended loop structures that append this structurally conserved core fold (Figure 1D,E) with an r.m.s.d. for alignment of all 215 Cα of 2.5 Å. Only the extended loop between β-strands 5 and 6 (Loop β5–β6) shows any significant structural variability and excluding this loop from the alignment reduces the r.m.s.d. to 1.8 Å for the remaining atom pairs. While this loop is similar in both molecules of KamB, with little defined secondary structure, for NpmA each copy of the protein possesses a distinct loop conformation that contains an α-helix (Supplementary Figure S2). In NpmA chain A, where this loop is more constrained by crystal packing contacts, it forms an extensive α-helix positioned closely against the rest of the protein with contacts to the adjacent short parallel α-helix of the loop between β-strands 4 and 5 (Loop β4–β5). Interactions are made to each end of the Loop β4–β5 helix, including a hydrogen bond between Glu146 and the peptide backbone of Gly108, and a salt bridge between Arg153 and Glu112 (Supplementary Figure S2). In contrast, in NpmA chain B where this loop is less restricted, the α-helix is shortened and the loop extends away from the core fold by up to 8 Å, disrupting these interactions. This apparent structural plasticity may be important for A1408 rRNA methyltransferase function (see 'Discussion' section).

The Rossmann-like Class I methyltransferase core fold is elaborated with two further additional structural motifs at the N-terminus and between β-strands 6 and 7 (Loop β6–β7; Figure 1E and Supplementary Figure S3). While the N-terminal β-hairpin is present in both structures and modestly conserved in sequence (Supplementary Figure S4), we do not believe it is likely to play a significant role in defining the function of the enzyme. In contrast, structural insertions between β-strands 6 and 7 are known to influence target selection and specificity in other Class I methyltransferases (11) and our structures and functional data, described below, suggest such a role for this extended loop in the A1408 rRNA methyltransferases.

Proteins of similar fold to KamB and NpmA were identified using the Dali server (25) and as expected the vast majority of retrieved structures were Class I methyltransferases (Z-score range 5.6–13.5). The greatest similarity was identified with the m^7G46 tRNA

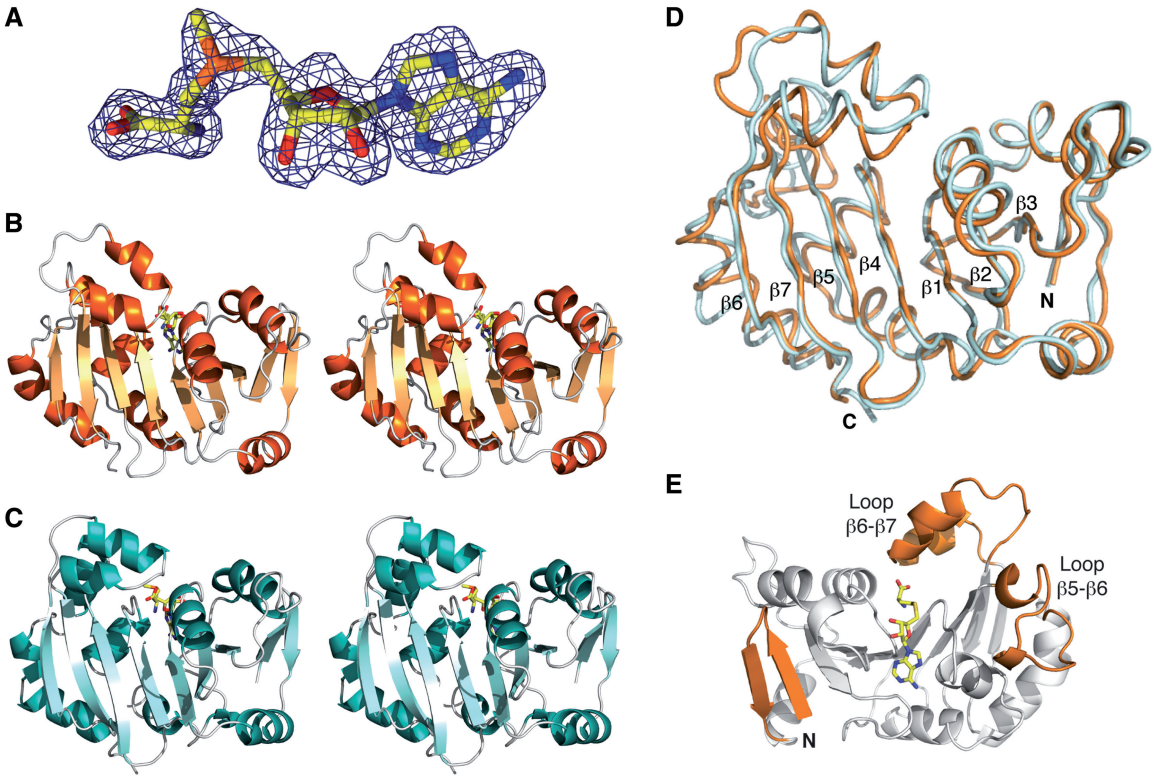

Figure 1. X-ray crystal structures of A1408 aminoglycoside-resistance rRNA methyltransferases. (**A**) SAM in omit $2F_o$–F_c electron density contoured at 1.0σ. Wall-eye stereo views of the (**B**) KamB–SAH and (**C**) NpmA–SAM complexes. Bound SAH or SAM molecules are shown as yellow sticks. (**D**) Alignment of KamB (orange) and NpmA (light cyan) crystal structures with β-strands of the Rossmann-like core SAM-dependent methyltransferase fold and the protein termini indicated. (**E**) Cartoon of the KamB–SAH complex with the three extended structural motifs on the core fold highlighted (orange). The view shown is rotated ~180° about the vertical axis from the orientation of panel B.

methyltransferases, with a clear top score for *Bacillus subtilis* TrmB (Z-score 16.2; PDB code 2FCA). Like the m^1A1408 methyltransferases, the m^7G46 tRNA methyltransferases possess a short N-terminal extension and a structurally similar Loop β6–β7 (Supplementary Figure S5). Thus these structures align very well (r.m.s.d. 2.7 Å). In contrast, the m^7G1405 aminoglycoside-resistance methyltransferase RmtB was ranked much lower in structural similarity, appearing on the list of retrieved structures well below many other Class I methyltransferases that modify tRNA, DNA, proteins or small molecules.

Critical residues for A1408 methyltransferase function

Using both the structures and amino acid conservation between KamB and NpmA as a guide, 22 putative key residues for A1408 methyltransferase function in SAM binding and target selection or modification were identified (Table 2). Each was individually mutated to alanine, with Trp105 and Trp193 additionally mutated to phenylalanine, and the mutant proteins tested for their ability to support bacterial growth in liquid culture in the presence of kanamycin (0–1200 μg/ml).

SAM binding. KamB and NpmA each contain a conserved GXGXG sequence (amino acids 32–36) within

Table 2. Mutagenesis and analysis of KamB activity in liquid culture

Proposed Function	Plasmid/ mutation	Kanamycin MIC (μg/ml)
Control	Empty pQE30	10
	pQE30–KamB	>1200
RNA/30S Binding	R8A	>1200
	K37A	50
	K58A	800
	K63A	800
	K67A	400
	K71A	400
	K74A	200
	K174A	>1200
	R179A	800
	R195A	400
	R196A	10
	R201A	10
	R203A	800
SAM binding	D30A	20
	D55A	10
	R60A	800
	E88A	400
	S107A	800
	T191A	10
A1408 Positioning/catalysis	W105A	10
	W105F	10
	N138A	100
	W193A	10
	W193F	10

their methyltransferase 'Motif I', that forms part of the SAM-binding site. In KamB, one additional residue from this motif, Asp30, forms a water-mediated hydrogen bond that positions the SAH terminal amino group, while the carboxylate is within hydrogen bonding distance of both Arg60 and Thr191 (Figure 2A). The adenine ring is enclosed on its Hoogsteen edge by Glu88 and Ser107. A very similar set of interactions defines the SAM-binding pocket in NpmA (Supplementary Figure S6). Mutations to alanine confirmed the critical nature of Asp30, Asp55 and Thr191 in forming the SAM-binding pocket through the inability of the mutant enzymes to support growth at even the lowest kanamycin concentrations tested (Table 2). The water-mediated interaction of Asp30 has been observed in structures of several methyltransferases that act on mRNA (PDB code 1RI4), tRNA (PDB code 3DXY) and DNA (PDB code 3MHT). Mutations at Arg60, Glu88 and Ser107 result in more modest reductions in the enzyme's ability to support bacterial growth in the presence of kanamycin. This suggests that hydrophobic stacking interactions are most significant in positioning the adenine moiety of SAM, or that precisely recognizing and positioning the nucleobase is less critical than for the ribose and methionine moieties.

Target recognition and methylation. The intact 30S subunit is the minimal substrate for methylation by A1408 methyltransferases (28), suggesting that these enzymes recognize one or more RNA structures that are formed or become adjacent only in the fully assembled subunit. Thirteen surface lysine and arginine residues in KamB were mutated to alanine to identify the protein surface that interacts directly with the 30S subunit. The mutated residues are distributed over several structural motifs in the protein, but most are clustered on a single surface forming an extended positively charged patch (Figure 2B). Two mutations, Arg8 and Lys174 to alanine, produced proteins with an activity indistinguishable from wild-type in the MIC assay. The former result suggests that the N-terminal β-hairpin extension to the core Rossmann-like fold is not critical for specific A1408 methyltransferase function. The majority of the mutated proteins confer a range of resistance levels with kanamycin MICs decreased at least 1.5- to 12-fold (Table 2). However, two mutant proteins with alanine substitutions at Arg196 and Arg201 confer no resistance to even the lowest kanamycin concentration (Table 2). This result clearly implicates these residues and the Loop β6–β7 extended structure as critical determinants of enzyme function such as rRNA recognition or specific target site selection.

Examination of the protein surface surrounding the bound coenzyme identified a pocket that might potentially accommodate A1408 adjacent to the methyl group for transfer. Two conserved tryptophans, 105 and 193, line this pocket (Figure 2A) and we hypothesized that they might play a role in the correct positioning of the target nucleoside. In support of this, mutation of either residue to alanine or, more conservatively, to phenylalanine completely abolished enzyme activity in the MIC assay (Table 2). We next used the HADDOCK webserver (26) to model an adenine nucleotide in the pocket between these two residues, which resulted in the positioning of adenine N1 3.7 Å from the methyl group of the modeled SAM (Figure 3). Similar experiments with larger fragments of helix 44 failed to produce a satisfactory positioning of the adenine N1 relative to the SAM methyl group (closest approach ~12 Å) indicating that A1408 must to be 'flipped' from helix 44 in order to be correctly positioned adjacent to the bound SAM for methyl group transfer. The model also suggests that one or both of these conserved Trp residues may serve as a platform to position the adenine ring in the enzyme active site. Trp193 is located in the extended Loop β6–β7 structure, adjacent to the critical Arg196, and could readily interact with A1408 (Figure 3). We also note that Trp107 in NpmA (equivalent to KamB Trp105), clearly adopts two distinct alternate conformations in chain A, where the adjacent flexible Loop β5–β6 is in the extended conformation, but not in chain B where the loop is more compact

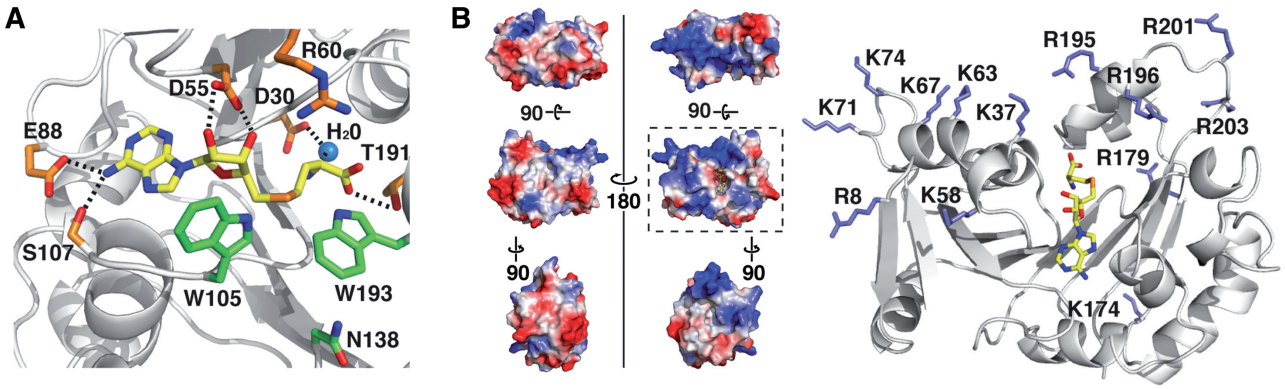

Figure 2. Critical residues for A1408 rRNA methyltransferase function. (**A**) Cartoon of the KamB structure surrounding the bound SAH. Residues proposed to be important for enzyme function through formation of the SAM-binding pocket (orange) or in A1408 target nucleotide positioning in the enzymatic center (green) are highlighted. (**B**) Multiple views of the KamB electrostatic surface representation (*left*) and cartoon (*right*) showing basic residues (blue) mutated to test their putative role in interaction with 30S ribosome subunit. The boxed surface orientation corresponds to the cartoon view (*left*). The coenzyme is modeled as SAH (yellow sticks). The effect of mutation at each indicated residue on kanamycin MICs is shown in Table 2.

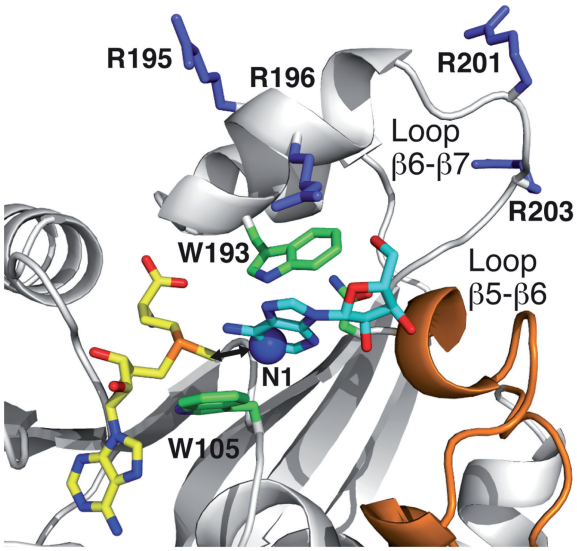

Figure 3. Model of A1408 bound in the KamB active site. An adenine nucleoside was docked into a surface pocket formed in part by the conserved and critical Trp105 and Trp193 residues. The adenine N1 is positioned 3.7 Å from the modeled methyl group (double arrow). Essential arginine residues 196 and 201 for A1408 methyltransferase activity in the adjacent extended structural motif in Loop β6–β7 are indicated and the flexible Loop β5–β6 is highlighted in orange.

(Supplementary Figures S2 and S7). Thus a number of plausible mechanisms can be envisaged by which specific target nucleotide selection might be coupled through dynamic changes in both protein and rRNA upon binding to activate the methyltransferase reaction (see 'Discussion' section)

One additional residue, Asn138, previously identified as having a potential role in catalysis (10), is also located adjacent to the modeled A1408 nucleotide. The KamB protein with an Asn138 to alanine mutation was indeed considerably less effective in the MIC assay (>12-fold reduced; Table 2). However, despite its proximity to the catalytic center, the residue is unlikely to be directly involved in the nucleobase modification reaction. The equivalent residue in NpmA is Thr140 and thus lacks the side chain amino group of Asn138 which is oriented toward the A1408 nucleobase in the modeled complex with KamB. However, a hydrogen bonding interaction with the amide backbone at Asp205 (Ser208 in NpmA) is conserved for both Asn138 and Thr140. Thus, the likely role of this residue is maintenance of a structurally critical interaction between the two extended structural motifs that define the functional specificity of the A1408 rRNA methyltransferases.

Sequence analysis corroborates the structural link to m^7G46 tRNA methyltransferases

The KamB and NpmA protein sequences were used as search subjects in FlowerPower (29), a clustering algorithm that can identify homologous sequences with similar domain architectures. The sequences retrieved were used in a BLAST search and a phylogenetic relatedness inferred for a subset of the returned sequences after reduction of sequence redundancy (Supplementary Figure S8). The maximum likelihood (ML) phylogenetic reconstruction showed a division of the analyzed sequences in two major clades: one comprising the m^1A1408 resistance methyltransferases and the second the m^7G46 tRNA methyltransferases. Thus the high structural relatedness identified via the Dali server using our KamB and NpmA structures is recapitulated by sequence analysis. Curiously, however, using the *B. subtilis* TrmB sequence in a reverse FlowerPower search failed to retrieve any aminoglycoside-resistance A1408 rRNA methyltransferase.

Finally, from our combined structure–function and sequence alignment analyses we can address the likelihood of putative A1408 methyltransferases (Supplementary Figures S1 and S8) to possesses this specific activity. While there are some exceptions, the majority of residues where mutation most affects enzyme activity are conserved in these proteins despite their relatively low sequence similarity (Supplementary Figure S4). Thus, our results add structure-function validation for the inclusion of these additional enzymes in the A1408 family and suggest that they are *bona fide* rRNA methyltransferases acting at A1408.

DISCUSSION

Despite their prevalence among antibiotic-producing bacteria and emergence in the last decade as a new threat to the clinical use of aminoglycosides, until recently few structural or functional details were known about the A1408 and G1405 families of resistance rRNA methyltransferases. However, initial modeling and mutagenesis studies on both families (10,30,31) were very recently followed by crystal structures of G1405 methyltransferases of pathogenic (16) and aminoglycoside-producer origin (17). The present studies complete the structural characterization of the second aminoglycoside-resistance rRNA methyltransferase family and allow direct comparison of the likely mechanisms of action between the two enzyme families.

As predicted by previous sequence analyses, both producer and pathogenic bacterial A1408 and G1405 aminoglycoside-resistance methyltransferases are Class I SAM-dependent methyltransferases. These enzymes all possess a characteristic Rossmann-like core SAM-binding fold (11). However, the structural embellishments around this core fold differ significantly between the G1405 and A1408 enzymes but are highly conserved within each family between enzymes of aminoglycoside-producer and pathogenic origin. The concept that aminoglycoside-resistance 16S rRNA methyltransferases found in pathogenic bacteria arose following horizontal transfer from an aminoglycoside-producer is clearly supported by this high structural conservation. However, with a G/C content of only 34%, the origin of the only currently known A1408 methyltransferase gene *npm*A appears unlikely to be the G/C-rich actinomycete, where ~70% G/C content is typical for known 16S rRNA methyltransferases. The A1408 methyltransferases show

strong structural similarity to m^7G46 tRNA methyltransferases outside of the core SAM-binding fold, suggesting the possibility that these enzymes evolved from a common ancestor, for example by gene duplication and divergence of methylation target. This link was corroborated in parallel using sequence-based searches with KamB and NpmA, but the reverse search using the tRNA modifying enzyme sequence did not retrieve any A1408 rRNA methyltransferase. This indicates that there is significant divergence from any such common ancestor and that these enzymes evolved independently in function while maintaining the overall protein fold. However, this observation does provide an alternative molecular evolutionary route to A1408 methyltransferases in pathogenic bacteria other than the direct horizontal transfer of a resistance enzyme from an aminoglycoside-producing strain.

The A1408 and G1405 methyltransferases do not methylate naked 16S rRNA, nor will they bind or methylate model helix 44 fragments despite the structural similarity of the isolated domain to the structure in the 30S subunit. Given the close proximity of the two target nucleotides, their respective methyltransferases must presumably recognize many of the same features of the 30S subunit architecture around helix 44 (Figure 4). Outside of their structurally conserved Class I methyltransferase SAM-binding domain core, the G1405 and A1408 enzymes differ significantly in structure (Figure 4). The G1405 methyltransferases are ~5 kDa larger and possess an extended N-terminal structure divided into two subdomains termed 'N1' and 'N2' (16). The enzyme activity is abolished in the absence of the N1 three-helix bundle and it is proposed that this domain is critical for binding 30S. In contrast, the A1408 methytransferases lack a large functionally important N-terminal extension and, instead, have extended structural motifs between β-strands 5 and 6, and β-strands 6 and 7. The latter structural motif, that was found here to contain three amino acids critical for A1408 methyltransferase function (Trp193, Arg196 and Arg201 in KamB), is completely absent in all examples of the G1405 methyltransferases structurally characterized to date. Thus the m^7G1405 and m^1A1408 methyltransferase families appear to employ substantially different mechanisms to recognize and select their target nucleotide.

Comparison of the KamB and NpmA structures allows us to speculate further on the mechanism of specific target selection for the A1408 methyltransferases. In the 30S subunit, A1408 is stacked in helix 44 opposite A1492 and A1493, such that the nucleobase would need to be 'flipped' into the enzyme active site, in common with several other nucleic acid modifying enzymes (32) and recently proposed for the G1405 resistance methyltransferases (17). Superposition of KamB onto the methyltransferase *Hha*I (PDB code 3MHT) (33) bound to DNA, positions the extended structural motif of Loop β5–β6 (residues 141–156) next to the major groove of the nucleic acid helix. We suggest that this loop structure directly contributes to recognition and flipping of the A1408 conformation, and that the structural plasticity we observe is important for this role. In the NpmA crystal, where this loop is unrestrained by packing contacts, it forms an extended structure with a short helix that could represent an initial recognition conformation. In contrast, when packed against the 30S surface the structure folds more compactly against the active site of the enzyme, mimicked by crystal packing contacts for NpmA chain A. Because this loop makes direct contacts

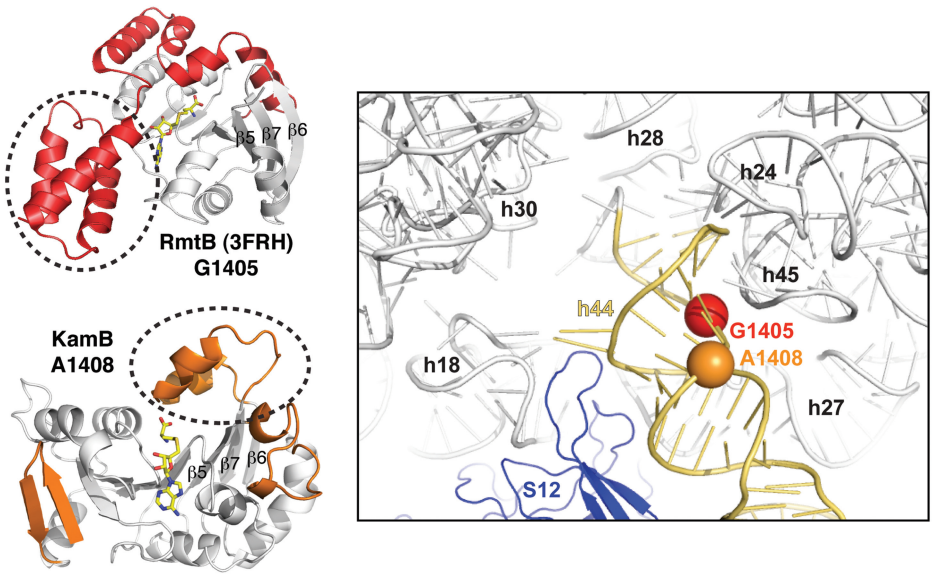

Figure 4. A1408 and G1405 aminoglycoside-resistance methyltransferases and their target sites in the 30S subunit. The distinct structural embellishments on the core Rossmann-like SAM binding core that define the structures of G1405 (red) and A1408 (orange) are highlighted on the RmtB (PDB code 3FRH) and KamB structures, respectively. *Right*, the methylation target sites shown surrounded by the common 30S architectural features that must be recognized by these enzymes. This surface is composed primarily of distant 16S rRNA helices, brought into proximity in the assembled 30S, and one ribosomal protein, S12.

with other regions of the protein implicated in target recognition (Loop β6–β7) and positioning the A1408 nucleobase (Trp105 in Loop β4–β5), a binding-induced conformational change could be relayed to activate methyltransfer. Indeed, the conformational restriction of the critical Trp105 (107 in NpmA) mirrors the changes in this loop structure. Thus, the differences in the SAM-bound NpmA may represent two relevant distinct conformational states of the protein during the recognition process. In this regard, it is noteworthy that in KamB, where the protein appears to be bound by the reaction by-product SAH, this loop is in a third distinct conformation with little secondary structure.

Many important questions remain regarding the specific details of the target recognition mechanisms for both families of aminoglycoside-resistance methyltransferases. This aspect of enzyme function is likely to most uniquely define their activity from other SAM-dependent methyltransferases. High-resolution structural characterization of these enzymes bound to their 30S ribosomal subunit target are thus urgently required to better define target recognition mechanisms before these broad aminoglycoside-resistance determinants proliferate further among pathogenic bacterial strains.

ACCESSION NUMBERS

3MQ2, 3MTE.

SUPPLEMENTARY DATA

Supplementary Data are available at NAR Online.

ACKNOWLEDGEMENTS

The authors thank the staff at SER-CAT beamlines ID22 and BM22 (Advanced Photon Source) for assistance with X-ray data collection and Dr Christine Dunham for comments on the manuscript.

FUNDING

National Institutes of Health (AI088025); Laboratory start-up funds from the Department of Biochemistry, Emory University School of Medicine. The authors thank Dr Ewan W. Blanch for assistance in managing the Wellcome Trust grant (079242) providing salary support for R.M. Funding for open access charge: National Institutes of Health/NIAID.

Conflict of interest statement. None declared.

REFERENCES

1. Jana,S. and Deb,J.K. (2006) Molecular understanding of aminoglycoside action and resistance. *Appl. Microbiol. Biotechnol.*, **70**, 140–150.
2. Noller,H.F. (1991) Ribosomal RNA and translation. *Annu. Rev. Biochem.*, **60**, 191–227.
3. Savic,M., Lovric,J., Tomic,T.I., Vasiljevic,B. and Conn,G.L. (2009) Determination of the target nucleosides for members of two families of 16S rRNA methyltransferases that confer resistance to partially overlapping groups of aminoglycoside antibiotics. *Nucleic Acids Res.*, **37**, 5420–5431.
4. Cundliffe,E. (1989) How antibiotic-producing organisms avoid suicide. *Annu. Rev. Microbiol.*, **43**, 207–233.
5. Long,K.S. and Vester,B. (2009) Antibiotic resistance in bacteria caused by modified nucleosides in 23S ribosomal RNA. In Grosjean,H. (ed.), *DNA and RNA Modification Enzymes: Comparative Structure, Mechanism, Functions, Cellular Interactions and Evolution*. Landes Bioscience, Austin, TX, pp. 537–549.
6. Conn,G.L., Savic,M. and Macmaster,R. (2009) Antibiotic resistance in bacteria through modification of nucleosides in 16S ribosomal RNA. In Grosjean,H. (ed.), *DNA and RNA Modification Enzymes: Comparative Structure, Mechanism, Functions, Cellular Interactions and Evolution*. Landes Bioscience, Austin, TX, pp. 524–536.
7. Gaynor,M. and Mankin,A.S. (2003) Macrolide antibiotics: binding site, mechanism of action, resistance. *Curr. Top. Med. Chem.*, **3**, 949–960.
8. Doi,Y. and Arakawa,Y. (2007) 16S ribosomal RNA methylation: emerging resistance mechanism against aminoglycosides. *Clin. Infect. Dis.*, **45**, 88–94.
9. Wachino,J., Shibayama,K., Kurokawa,H., Kimura,K., Yamane,K., Suzuki,S., Shibata,N., Ike,Y. and Arakawa,Y. (2007) Novel plasmid-mediated 16S rRNA m1A1408 methyltransferase, NpmA, found in a clinically isolated Escherichia coli strain resistant to structurally diverse aminoglycosides. *Antimicrob. Agents Chemother.*, **51**, 4401–4409.
10. Koscinski,L., Feder,M. and Bujnicki,J.M. (2007) Identification of a missing sequence and functionally important residues of 16S rRNA: m(1)A1408 methyltransferase KamB that causes bacterial resistance to aminoglycoside antibiotics. *Cell Cycle*, **6**, 1268–1271.
11. Schubert,H.L., Blumenthal,R.M. and Cheng,X.D. (2003) Many paths to methyltransfer: a chronicle of convergence. *Trends Biochem. Sci.*, **28**, 329–335.
12. Felnagle,E.A., Rondon,M.R., Berti,A.D., Crosby,H.A. and Thomas,M.G. (2007) Identification of the biosynthetic gene cluster and an additional gene for resistance to the antituberculosis drug capreomycin. *Appl. Environ. Microbiol.*, **73**, 4162–4170.
13. Zhao,J.Y., Xia,Z.J., Sun,X., Zhong,L., Jiang,D.M., Liu,H., Wang,J., Qin,Z.J. and Li,Y.Z. (2008) Cloning and characterization of an rRNA methyltransferase from Sorangium cellulosum. *Biochem. Biophys. Res. Comm.*, **370**, 140–144.
14. Holmes,D.J., Drocourt,D., Tiraby,G. and Cundliffe,E. (1991) Cloning of an aminoglycoside-resistance-encoding gene, kamC, from Saccharopolyspora hirsuta: comparison with kamB from Streptomyces tenebrarius. *Gene*, **102**, 19–26.
15. Tamura,T., Ishida,Y., Otoguro,M., Hatano,K. and Suzuki,K. (2008) Classification of 'Streptomyces tenebrarius' Higgins and Kastner as Streptoalloteichus tenebrarius nom. rev., comb. nov., and emended description of the genus Streptoalloteichus. *Int. J. Syst. Evol. Microbiol.*, **58**, 688–691.
16. Schmitt,E., Galimand,M., Panvert,M., Courvalin,P. and Mechulam,Y. (2009) Structural bases for 16S rRNA methylation catalyzed by ArmA and RmtB methyltransferases. *J. Mol. Biol.*, **388**, 570–582.
17. Husain,N., Tkaczuk,K.L., Tulsidas,S.R., Kaminska,K.H., Cubrilo,S., Maravic-Vlahovicek,G., Bujnicki,J.M. and Sivaraman,J. (2010) Structural basis for the methylation of G1405 in 16S rRNA by aminoglycoside resistance methyltransferase Sgm from an antibiotic producer: a diversity of active sites in m7G methyltransferases. *Nucleic Acids Res.*, doi:10.1093/nar/gkq1122.
18. Otwinowski,Z. and Minor,W. (1997) Processing of X-ray diffraction data collected in oscillation mode. *Methods in Enzymology*, **276**, 307–326.
19. Zwart,P.H., Afonine,P.V., Grosse-Kunstleve,R.W., Hung,L.W., Ioerger,T.R., McCoy,A.J., McKee,E., Moriarty,N.W., Read,R.J., Sacchettini,J.C. *et al.* (2008) Automated structure solution with the PHENIX suite. *Methods Mol. Biol.*, **426**, 419–435.
20. Langer,G., Cohen,S.X., Lamzin,V.S. and Perrakis,A. (2008) Automated macromolecular model building for X-ray crystallography using ARP/wARP version 7. *Nat. Protoc.*, **3**, 1171–1179.

21. Emsley,P. and Cowtan,K. (2004) Coot: model-building tools for molecular graphics. *Acta Crystallogr.*, **D60**, 2126–2132.
22. McCoy,A.J., Grosse-Kunstleve,R.W., Adams,P.D., Winn,M.D., Storoni,L.C. and Read,R.J. (2007) Phaser crystallographic software. *J. Appl. Crystallogr.*, **40**, 658–674.
23. Adams,P.D., Gopal,K., Grosse-Kunstleve,R.W., Hung,L.W., Ioerger,T.R., McCoy,A.J., Moriarty,N.W., Pai,R.K., Read,R.J., Romo,T.D. *et al.* (2004) Recent developments in the PHENIX software for automated crystallographic structure determination. *J. Synchrotron. Radiat.*, **11**, 53–55.
24. Painter,J. and Merritt,E.A. (2006) TLSMD web server for the generation of multi-group TLS models. *J. Appl. Crystallogr.*, **39**, 109–111.
25. Holm,L. and Sander,C. (1995) Dali: a network tool for protein structure comparison. *Trends Biochem Sci*, **20**, 478–480.
26. de Vries,S.J., van Dijk,A.D., Krzeminski,M., van Dijk,M., Thureau,A., Hsu,V., Wassenaar,T. and Bonvin,A.M. (2007) HADDOCK versus HADDOCK: new features and performance of HADDOCK2.0 on the CAPRI targets. *Proteins*, **69**, 726–733.
27. Dunstan,M.S., Hang,P.C., Zelinskaya,N.V., Honek,J.F. and Conn,G.L. (2009) Structure of the thiostrepton resistance methyltransferase-S-adenosyl-L-methionine complex and its interaction with ribosomal RNA. *J. Biol. Chem.*, **284**, 17013–17020.
28. Douthwaite,S., Fourmy,D. and Yoshizawa,S. (2005) In Grosjean,H. (ed.), *Fine-Tuning of RNA Funtions by Modification and Editing*, Vol. 12. Springer-Verlag, Berlin, pp. 285–307.
29. Krishnamurthy,N., Brown,D. and Sjolander,K. (2007) FlowerPower: clustering proteins into domain architecture classes for phylogenomic inference of protein function. *BMC Evol. Biol.*, **7(Suppl. 1)**, S12.
30. Savic,M., Ilic-Tomic,T., Macmaster,R., Vasiljevic,B. and Conn,G.L. (2008) Critical residues for cofactor binding and catalytic activity in the aminoglycoside resistance methyltransferase Sgm. *J. Bacteriol.*, **190**, 5855–5861.
31. Vlahovicek,G.M., Cubrilo,S., Tkaczuk,K.L. and Bujnicki,J.M. (2008) Modeling and experimental analyses reveal a two-domain structure and amino acids important for the activity of aminoglycoside resistance methyltransferase Sgm. *Biochim. Biophys. Acta, Proteins Proteomics*, **1784**, 582–590.
32. Cheng,X. and Blumenthal,R.M. (2002) Cytosines do it, thymines do it, even pseudouridines do it - base flipping by an enzyme that acts on RNA. *Structure*, **10**, 127–129.
33. O'gara,M., Horton,J.R., Roberts,R.J. and Cheng,X.D. (1998) Structures of Hhal methyltransferase complexed with substrates containing mismatches at the target base. *Nat. Struct. Biol.*, **5**, 872–877.